Structure of HIV-1 RT/TIBO R 86183 complex reveals similarity in the binding of diverse nonnucleoside inhibitors

Jianping Ding[1], Kalyan Das[1], Henri Moereels[2], Luc Koymans[2], Koen Andries[2], Paul A.J. Janssen[2], Stephen H. Hughes[3] and Edward Arnold[1]

We report the structure of HIV-1 reverse transcriptase (RT) complexed with the nonnucleoside inhibitor TIBO R 86183 at 3.0 Å resolution. Comparing this structure with those of complexes of HIV-1 RT/α-APA R 95845 and HIV-1 RT/nevirapine provides a basis for understanding the nature of nonnucleoside inhibitor binding, the structure of the binding site and the interactions between the bound inhibitors and surrounding amino acid residues as well as for understanding mechanisms of inhibition by and resistance to nonnucleoside inhibitors. All three inhibitors considered assume a similar butterfly-like shape and bind to HIV-1 RT in a very similar way. Important differences occur in the conformation of amino acid residues that form the binding pocket.

[1]Center for Advanced Biotechnology and Medicine (CABM) and Rutgers University Chemistry Department, 679 Hoes Lane, Piscataway, New Jersey 08854-5638, USA
[2]Janssen Research Foundation, Turnhoutseweg 30, B-2340 Beerse, Belgium
[3]ABL-Basic Research Program, NCI-Frederick Cancer Research and Development Center, P.O. Box B, Frederick, Maryland 21702-1201, USA

J.D. and K.D contributed equally to this work.

Correspondence should be addressed to E.A.

The reverse transcriptase (RT) of human immunodeficiency virus type 1 (HIV-1) is essential for replication of the AIDS virus. Currently two classes of anti-AIDS chemotherapeutic agents have been developed which target this enzyme[1]. 3'-azido-2',3'-dideoxythymidine (AZT), 2',3'-dideoxyinosine (ddI), 2',3'-dideoxycytidine (ddC), and 2',3'-didehydro-2',3'-dideoxythymidine (d4T) are nucleoside analogues which have been approved for the treatment of HIV-1 infection. The nonnucleoside inhibitors include tetrahydro-imidazo(4,5,1-*jk*) (1,4)-benzodiazepin-2(*1H*)-one and -thione (TIBO) derivatives[2], 11-cyclopropyl-5,11-dihydro-4-methyl-6H-dipyrido(3,2-b:2',3'-e)(1,4)diazepin-6-one (BI-RG-587 or nevirapine)[3], pyridinones[4], α-anilinophenylacetamide (α-APA) derivatives[5], and bis(heteroaryl)piperazine (BHAP) derivatives[6] (reviewed in refs 7–9)(Fig. 1). These and other nonnucleoside inhibitors are chemically and structurally diverse, but they are all specific for HIV-1 RT and functionally noncompetitive with respect to nucleotide incorporation[3,4,10–14].

The TIBO compounds were the first class of nonnucleoside HIV-1 RT inhibitors to be described[2]. An 8-chloro substituted derivative, TIBO R 86183 (Fig. 1) is particularly potent. TIBO R 86183 has an EC_{50} (concentration of compound protecting 50 % of MT-4 cells against HIV-1-induced cytopathic effects) of 4 nM, a CC_{50} (concentration of compound causing 50 % cytotoxicity) of 77 mM, and a selectivity index (ratio of CC_{50} to EC_{50}) of 19,250 (ref. 15). A noteworthy feature of TIBO R 86183 is that it is potent in inhibiting the Y181C mutant of HIV-1 RT (ref. 15). This mutation has been commonly observed in both cell culture and clinical studies of HIV-1 infection with numerous nonnucleoside inhibitors, and confers a high degree of resistance to most of them, including α-APA, nevirapine and other TIBO derivatives.

The crystal structure at 2.9 Å resolution of HIV-1 RT complexed with nevirapine showed that the inhibitor binds to a hydrophobic pocket which is close, but distinct from, the polymerase active site[16,17]. We have recently solved the crystal structure of HIV-1 RT complexed with the nonnucleoside inhibitor α-APA R 95845 at 2.8 Å resolution[18]. This paper reports the crystal structure of HIV-1 RT complexed with TIBO R 86183 at 3.0 Å resolution. A detailed comparison of the nonnucleoside inhibitor-binding pockets (NNIBP), the geometry of bound inhibitors and the interactions between protein and inhibitors in the three structures revealed that there is a striking similarity in the binding mode of these diverse nonnucleoside inhibitors. These observations may have implications for the design of improved nonnucleoside inhibitors.

NNIBP and protein-inhibitor interactions

The crystals of the HIV-1 RT/TIBO, HIV-1 RT/α-APA, and HIV-1 RT/nevirapine complexes are nearly isomorphous, and are of the monoclinic space group C2. An asymmetric unit contains one HIV-1 RT p66/p51 heterodimer and one inhibitor molecule. The overall folding of the HIV-1 RT p66/p51 heterodimer in these three complexes is similar. The polymerase domains of both p66 and p51 subunits contain identical amino acid sequences and fold into similar subdomains which are called fingers, palm, thumb and connection (for recent

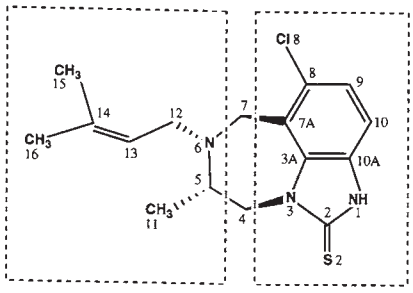

TIBO R 86183

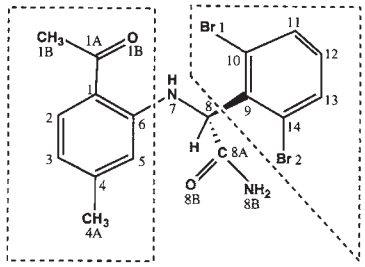

(−) α-APA R 95845

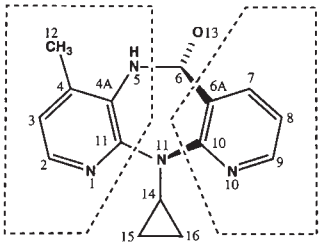

Nevirapine

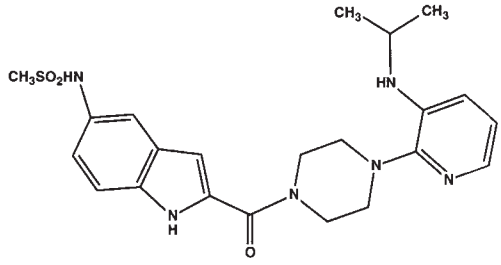

BHAP U-90152S

Fig. 1 Chemical structures of nonnucleoside inhibitors: 8-Cl-tetrahydro-imidazo(4,5,1-*jk*)(1,4)-benzodiazepin-2-one (TIBO R 86183), α-anilinophenylacetamide (α-APA R 95845) and dipyridodiazepinone (nevirapine). The moieties contained in the dashed boxes correspond to the Wing I (left) and Wing II (right) segments of the butterfly-like shape analogy. For comparison, the chemical structure of bis(heteroaryl)piperazine (BHAP U-90152S) is also shown.

review see ref.19). The overall arrangement of individual subdomains in the two subunits is different[16,20]. The C-terminal portion of p66 forms the RNase H domain. The fingers, palm and thumb subdomains of p66 form a large cleft that binds the template-primer nucleic acid[20]. In the absence of nucleic acid, the p66 thumb subdomain is folded down into the DNA-binding cleft (Arnold, E. *et al.*, unpublished observations refs 21, 22). Binding of nonnucleoside inhibitors, however, is sufficient to cause the p66 thumb to adopt a conformation similar to that seen in the DNA-bound HIV-1 RT structure[16,18]. The polymerase active site is located at the palm subdomain of p66 and contains three conserved aspartic acid residues (Asp 110, Asp 185 and Asp 186) which lie on the 'floor' of the DNA-binding cleft.

As in the known HIV-1 RT/nonnucleoside inhibitor complex structures[16,18], the nonnucleoside inhibitor in the HIV-1 RT/TIBO R 86183 complex structure is also located in the NNIBP (Fig. 2). A putative entrance to the pocket is formed primarily by amino acid residues Leu 100, Lys 101, Lys 103, Val 179 and Tyr 181 of p66, and Glu 138 of the β7-β8 loop of p51. This entrance is relatively narrow compared to the size of an inhibitor and is open towards the interface of the p66/p51 heterodimer. Although nonnucleoside inhibitors are structurally diverse, all are hydrophobic and contain aromatic groups. Since most of the residues that form the NNIBP are also hydrophobic, the interactions between the amino acid residues of the pocket and the bound inhibitors are predominantly hydrophobic (Table 1). Interactions between the aromatic groups of inhibitors and those of amino acid residues in the binding pocket, especially Tyr 181, Tyr 188 and Trp 229, play an important role in stabilizing the binding of nonnucleoside inhibitors[18,23]. On the other hand, most of the nonnucleoside inhibitors also contain polar groups (NH or NH_2, for example) which have the potential to form hydrogen bonds with the surrounding residues. In the HIV-1 RT/α-APA complex, the amide group (N8B) of α-APA forms hydrogen bonds with the main-chain carbonyl oxygen atoms of Tyr 188 and Val 189. In the HIV-1 RT/TIBO complex, the amine group (N1) of TIBO forms a hydrogen bond with the main-chain carbonyl oxygen atom of Lys 101. These hydrogen-bonding interactions may be important in precisely positioning the inhibitors in the pocket. No hydrogen bonds were observed between nevirapine and the protein in the HIV-1 RT/nevirapine complex[17].

It is possible that bound water molecules also interact with polar atoms of both the protein and the bound inhibitors. There is good evidence that some residual electron density exists in and around the NNIBP in difference Fourier maps with reasonable stereochemistry for water molecules that could bridge inhibitor and protein atoms, but the present resolution of these structures does not permit accurate location of water molecules.

An electron density peak that was consistently present in difference Fourier maps for the HIV-1 RT/α-APA complex is located near the entrance to the pocket with reasonable density height and stereochemistry for a water molecule (at a distance of 3.6 Å from the oxygen atom O1B of the acetyl group of the inhibitor and 3.3 Å from Oε1 of Glu 138 of p51). Peaks of similar significance were found in the difference Fourier electron density maps for the HIV-1 RT/TIBO complex near the entrance of the pocket, but none of the nearby atoms of TIBO R 86183 are polar, so potential hydrogen bonds would be with protein atoms only in that structure.

An important difference between the chemical structures of the TIBO derivatives and those of α-APA and nevirapine is that TIBO compounds contain only one aromatic group, whereas the other two have two distinct aromatic rings. As with other nonnucleoside inhibitors, mutations of either Tyr 181 or Tyr 188 significantly affect the sensitivity of HIV-1 RT to many TIBO derivatives (albeit to a lesser extent with TIBO R

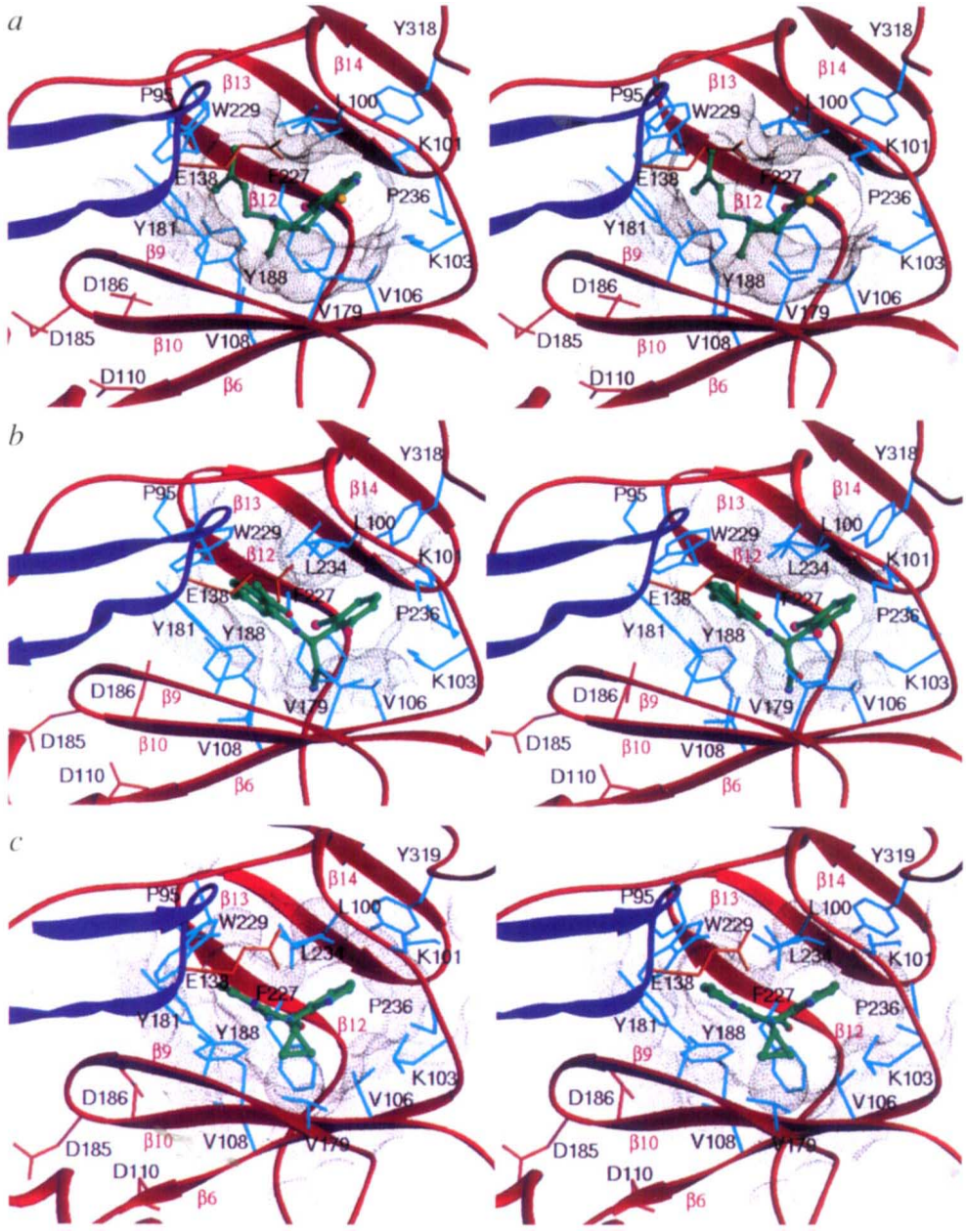

Fig. 2 Ribbon diagram[31] showing the structures of the nonnucleoside inhibitor-binding pocket and the interactions between inhibitors and surrounding amino acid residues in *a*, the HIV-1 RT/TIBO R 86183, *b*, the HIV-1 RT/α-APA R 95845 and *c*, the HIV-1 RT/nevirapine complexes. All three complexes are shown in the same orientation looking through a putative entrance to the pocket. The secondary structural elements which form the NNIBP are shown as ribbons with those from p66 in red and p51 in blue. The inhibitors are shown in ball-and-stick models with carbons green, nitrogens blue, oxygens red, sulphurs yellow and halogens magenta. The side chains are shown for the amino acid residues which form the inner surface of the pocket and make close contacts with the inhibitors and those of three aspartic acids at the catalytic active-site. The dotted surface delineates the solvent-accessible cavity of the NNIBP.

86183), so it was anticipated that the aromatic moiety of TIBO R 86183 would interact with the aromatic side chains of Tyr 181 and Tyr 188. Favourable aromatic–aromatic interactions involving the side chains of Tyr 181 and Tyr 188 were observed in the structures of both HIV-1 RT/nevirapine and HIV-1 RT/α-APA complexes[17,18]. Surprisingly, the aromatic moiety of TIBO R 86183 does not make significant interactions with Tyr 181 or Tyr 188, but instead interacts with Leu 100, Lys 101, Val 179 and Tyr 318. The dimethylallyl aliphatic group of R 86183 interacts with Tyr 181, Tyr 188 and Trp 229.

Conformational changes create the NNIBP

Comparison of the crystal structures of the HIV-1 RT/nonnucleoside inhibitor complexes and the structures of HIV-1 RT in the absence of inhibitors reveals no significant change in the assignments of secondary structures around the NNIBP. Significant changes do occur in the orientations of the side chains of some residues and in the relative positions of the secondary structural elements. In the HIV-1 RT/DNA/Fab (ref. 20), HIV-1 RT/Fab (Arnold, E. *et al.*, unpublished observations) and the unliganded HIV-1 RT (ref. 22) structures, the side chains of Tyr 181 and Tyr 188 of p66 point into the hydrophobic core and, as a consequence, the NNIBP does not exist. Instead a surface depression is present at a location which is equivalent to the putative entrance of the pocket (Fig. 3). This surface depression is surrounded by residues Leu 100, Lys 101, Lys 103, Val 179, Tyr 181 and Tyr 188 of p66, and Glu 138 of p51. In the struc-

tures that have a bound nonnucleoside inhibitor, the side chains of both Tyr 181 and Tyr 188 are rotated away from their positions in the hydrophobic core, compared to the structures without bound inhibitor, and point toward the polymerase active site (Fig. 2). The side chain torsion angles (χ_1) of both Tyr 181 and Tyr 188 differ by about 120° in the structures derived in the presence and absence of inhibitors. As a result of these rotations, a space is created in the hydrophobic core to accommodate the nonnucleoside inhibitor. The major difference in the location of the secondary structural elements that form the pocket between the structures of HIV-1 RT with or without inhibitor is a differential twisting (about 30°) of the β12-β13-β14 sheet, which results in an expansion of the NNIBP. In the HIV-1 RT/inhibitor complexes, the side chains of Tyr 181 and Tyr 188 occupy approximately the position where the side chain of Trp 229 is found in the structures of HIV-1 RT obtained in the absence of inhibitors. Trp 229, which is located on the β12-β13 loop, is about 3 Å away from its position in the HIV-1 RT structures obtained in the absence of inhibitors. The β13-β14 loop, which contains Pro 236, is about 3 Å closer to the bound inhibitors relative to its position in the HIV-1 RT structures that do not contain inhibitor. In addition, the connecting loop of β5a and β6 (residues 95–102) is positioned outward from the pocket by about 2 Å in the HIV-1 RT/inhibitor complexes with respect to its position in the HIV-1 RT structures that lack the inhibitor, further enlarging the space of the NNIBP. The side chains of the residues at the rim of the putative entrance to the pocket have comparable orientations in all of the structures.

Although the binding pocket is hydrophobic, there are three hydrophilic residues (Lys 101 and Lys 103 of p66, and Glu 138 of p51) which are all located at the entrance. Mutations in any of these residues confer resistance to nonnucleoside inhibitors, suggesting that these residues affect the binding of nonnucleoside inhibitors and/or the structure of the NNIBP. The roles of these residues in binding nonnucleoside inhibitors are not yet clear. It is possible that the flexible and polar side chains of these hydrophilic residues may help steer the inhibitor molecule into the NNIBP.

Table 1 Distances (Å) between atoms of amino acid residues and inhibitors in the NNIBP (≤3.8 Å)

Residue	HIV-1 RT/TIBO	HIV-1 RT/α-APA	HIV-1 RT/nevirapine
L100	Cβ:N1, 3.4; Cδ1:C10, 3.7; Cδ1:C10A, 3.7	Cδ1:C1, 3.6; Cδ1:C1A, 3.7; Cδ1:C4A, 3.8; Cδ2:C1B, 3.7	Cγ:N1, 3.5; Cγ:C2, 3.6; Cδ1:C2, 3.8; Cδ2:N1, 3.3; Cδ2:C2, 3.4; Cδ2:C3, 3.4; Cδ2:C4, 3.5; Cδ2:C4A, 3.6; Cδ2:C11, 3.4
K101	O:N1, 2.6[1]; O:C2, 3.7; O:C10A, 3.6	O:C13, 3.5	O:C9, 3.3; O:N10, 3.6
K103		Cγ:Br2, 3.8	Cγ:C15, 3.8
V106		Cγ1:N8B, 3.2; Cγ1:Br1, 3.6; Cγ2:N8B, 3.7	Cγ2:C6, 3.8; Cγ2:O13, 3.2
V179	O:C11, 3.8; Cγ1:S2, 3.8; Cγ1:C4, 3.5; Cγ1:C11, 3.7	O:O8B, 3.4; Cβ:O8B, 3.6; Cγ1:O1B, 3.6; Cγ1:O8B, 3.7; Cγ1:Br2, 3.8	
Y181	N:C11, 3.5; Cβ:C11, 3.4; Cβ:C12, 3.5; Cγ:C12, 3.8	Cβ:C1, 3.6; Cβ:C1A, 3.6; Cγ:C1, 3.4; Cγ:C1A, 3.6; Cγ:C2, 3.3; Cδ1:C1B, 3.5; Cδ1:C2, 3.8; Cδ2:C1, 3.5; Cδ2:C2, 3.1; Cδ2:C3, 3.1; Cδ2:C4, 3.6; Cε2:C2, 3.3; Cε2:C3, 3.1; Cζ:C2, 3.7; Cγ:C1B, 3.8	Cβ:C2, 3.7; Cγ:C2, 3.7
Y188	O:C11, 3.2; Cβ:C12, 3.4; Cγ:C12, 3.7; Cγ:C16, 3.8; Cδ2:CL8, 3.6; Cδ2:C12, 3.5; Cδ2:C16, 3.5; Cε2:CL8, 3.8; Cε2:C16, 3.4; Cζ:C16, 3.7	C:N8B, 3.1; O:N8B, 2.8[1]; O:C8A, 3.5; O:O8B, 3.8; Cα:N8B, 3.8; Cβ:N8B, 3.3; Cδ2:C4A, 3.6; Cδ2:C5, 3.7; Cδ2:Br1, 3.7; Cε2:C4A, 3.3; Cζ:C4A, 3.8	O:C14, 3.8; O:C15, 3.7; O:C16, 2.7; C:C16, 3.8; Cβ:C4A, 3.7; Cβ:N5, 3.5; Cγ:N5, 3.7; Cδ2:N5, 3.3; Cδ2:C12, 3.8
V189		C:N8B, 3.2; O:N8B, 3.2[1]; N:N8B, 3.7	
G190		N:N8B, 3.3; N:O8B, 3.7; Cα:N8B, 3.5; Cα:O8B, 3.6	N:C15, 3.7; Cα:C15, 3.8
F227	Cδ2:CL8, 3.8		Cδ2:O13, 3.7; Cε2:O13, 3.7
W229	Cγ:C16, 3.8; Cδ1:C16, 3.8; Cδ2:C15, 3.7; Cδ2:C16, 3.7; Cε2:C15, 3.8; Cε2:C16, 3.7; Cε3:C15, 3.4; Nε1:C16, 3.7; Cζ2:C15, 3.7; Cζ3:C15, 3.2; Cη2:C15, 3.3	Cβ:C4A, 3.6; Cγ:C4A, 3.1; Cδ1:C4A, 3.7; Cδ2:C3, 3.6; Cδ2:C4, 3.7; Cδ2:C4A, 3.0; Cε2:C3, 3.4; Cε2:C4A, 3.5; Cε3:C3, 3.6; Cε3:C4, 3.7; Cε3:C4A, 3.3; Cζ2:C3, 3.2; Cζ3:C3, 3.4; Cη2:C2, 3.7; Cη2:C3, 3.2	Cγ:C12, 3.7; Cδ2:C12, 3.5; Cε2:C12, 3.7
L234		Cδ1:C4A, 3.8	Cδ1:N5, 3.5; Cδ1:C6, 3.5; Cδ1:C12, 3.4; Cδ1:O13, 3.6
H235		O:C11, 3.8; O:C12, 3.7	
P236			Cα:C8,3.6
Y318[2]	Cζ:C10, 3.7; Oη:C9, 3.6; Oη:C10, 3.6	Cε2:C11, 3.8; Cε2:C12, 3.0; Cε2:C13, 3.6; Cζ:C12, 3.8; Oη:C11, 3.7; Oη:C12, 3.7	Cε2:C8, 3.5; Cζ:C8, 3.7; Oη:C7, 3.8; Oη:C8, 3.6

[1]These atoms are involved in potential hydrogen-bonding interactions.
[2]In the HIV-1 RT/nevirapine complex, this residue is Tyr 319.

A butterfly-like shape

A comparison of the HIV-1 RT/TIBO, HIV-1 RT/α-APA[18] and HIV-1 RT/nevirapine[16,17] structures reveals striking similarities in the geometry of both the NNIBP and inhibitors. The three structures were superimposed based on the Cα atoms in the NNIBP region (β5a–β6: 92–112, β9–β10: 178–192, and β12–β14: 223–241); the root-mean-square deviations for 55 Cα atoms is 0.6 Å for the HIV-1 RT/TIBO and HIV-1 RT/α-APA comparison, 0.9 Å for the HIV-1 RT/TIBO and HIV-1 RT/nevirapine comparison, and 0.9 Å for the HIV-1 RT/α-APA and HIV-1 RT/nevirapine comparison. Despite these similarities there are conformational differences in the orientations of some side chains. The major difference in the conformation

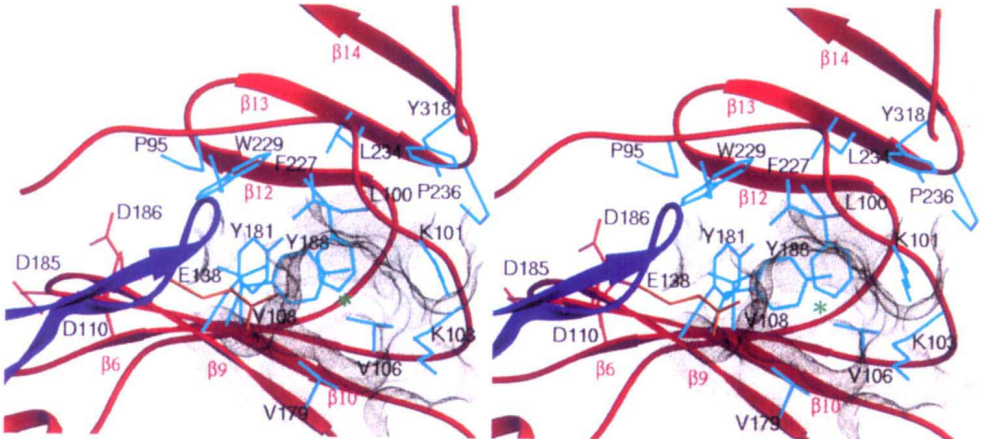

Fig. 3 Stereoview showing the region equivalent to the nonnucleoside inhibitor-binding pocket in the structure of the HIV-1 RT/DNA/Fab ternary complex[20]. The green star denotes the location of the surface depression and the dotted surface represents the solvent-accessible surface of the putative entrance to the pocket. The side chains of both Tyr 181 and Tyr 188 point into the hydrophobic core and the NNIBP does not exist. This orientation is approximately the same as that used in Fig. 2, but is slightly tilted to optimally view the pocket entrance and the surface depression.

compared with the α-APA complex structure.

There is a discrepancy between the HIV-1 RT/nevirapine complex and the HIV-1 RT/TIBO and HIV-1 RT/α-APA complexes in the positions of Tyr 318 and Tyr 319. In the HIV-1 RT/nevirapine structure, Tyr 319 points toward the pocket, while in the HIV-1 RT/TIBO and HIV-1 RT/α-APA complexes, Tyr 318, instead of Tyr 319, points toward the pocket. (The residue assignments between 314 and 336 in both the p66 and p51 subunits in the HIV-1 RT/nevirapine complex differ by one residue from that in the HIV-1 RT/α-APA and HIV-1 RT/TIBO complexes. The latter assignment was initially guided by the reference structure of unliganded HIV-1 RT[22] and was found to be correct on the basis of omit electron density maps and model refinement). In addition, there are differences in the side chain conformations of Val 106, Val 108 and Trp 229 in the HIV-1 RT/nevirapine complex and those in the HIV-1 RT/TIBO

of side chains in the NNIBP between the HIV-1 RT/TIBO and HIV-1 RT/α-APA complexes involves Tyr 318. The side chain of this residue is rotated by about 90° around torsion angle χ_2 if the TIBO complex structure is

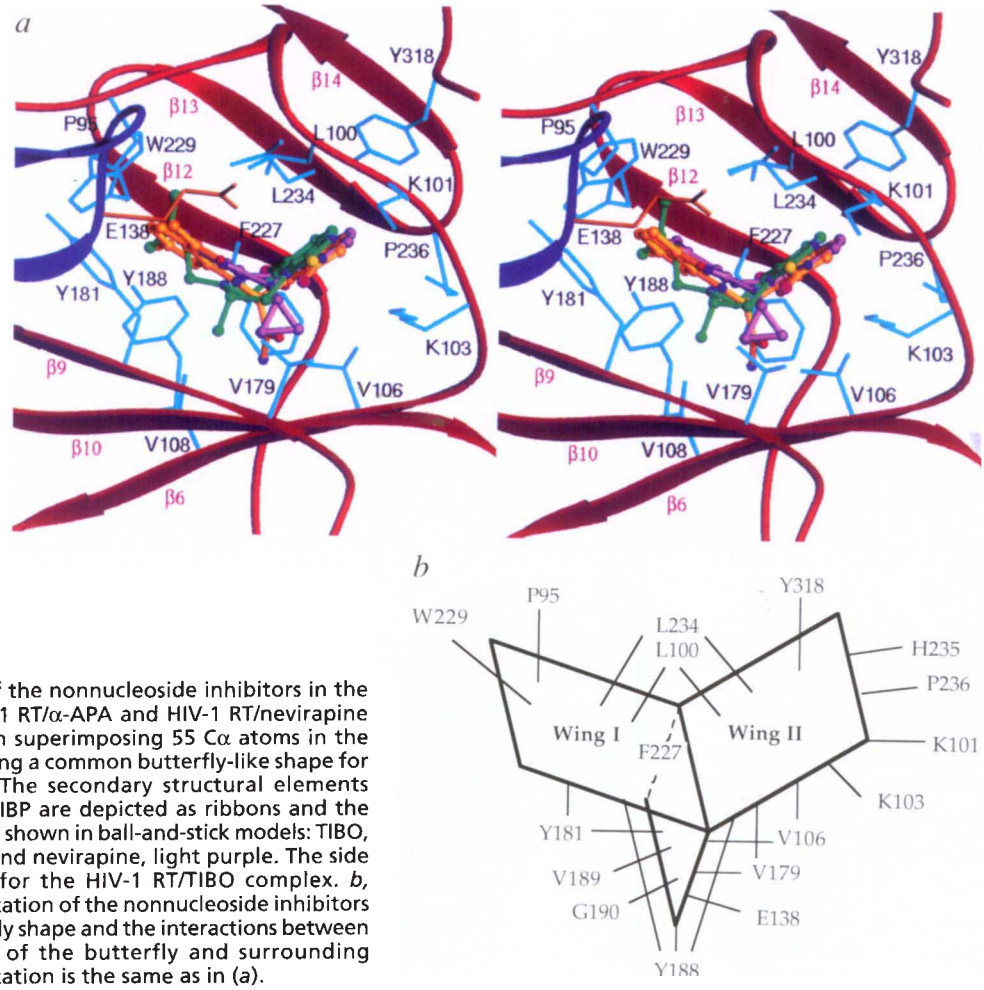

Fig. 4 *a*, Overlap of the nonnucleoside inhibitors in the HIV-1 RT/TIBO, HIV-1 RT/α-APA and HIV-1 RT/nevirapine complexes based on superimposing 55 Cα atoms in the NNIBP region showing a common butterfly-like shape for inhibitor binding. The secondary structural elements which form the NNIBP are depicted as ribbons and the bound inhibitors are shown in ball-and-stick models: TIBO, green, α-APA, red and nevirapine, light purple. The side chains are shown for the HIV-1 RT/TIBO complex. *b*, Schematic representation of the nonnucleoside inhibitors showing the butterfly shape and the interactions between different portions of the butterfly and surrounding residues. The orientation is the same as in (*a*).

and HIV-1 RT/α-APA complexes. The side chain of Val 179 in the HIV-1 RT/nevirapine complex points outward from the pocket and makes no contact with nevirapine, while the side chain of Val 179 in the HIV-1 RT/TIBO and HIV-1 RT/α-APA complexes points toward the pocket and makes hydrophobic interactions with bound inhibitors (Fig. 2 and Table 1).

Superimposition of the HIV-1 RT/TIBO, HIV-1 RT/α-APA and HIV-1 RT/nevirapine complexes based on the positions of secondary structural elements that form the NNIBP reveals that all three inhibitors occupy the same binding site. Both the inhibitors and the solvent accessible cavity of the NNIBP adopt a similar butterfly-like shape (Figs 2, 4). The long axis of these inhibitors is aligned along the β9-β10 hairpin. If we define the portion of the inhibitor that lies close to the polymerase active site as wing I and the other portion which is distal as wing II, the angle between the two wings is approximately 110-115° (TIBO: 112°, α-APA: 112°, and nevirapine: 115°). For TIBO, wing I contains the dimethylallyl aliphatic side group and a part of the seven-membered ring to which it is attached; wing II contains the benzodiazepinone moiety (Fig. 1). For α-APA, wing I consists of the substituted α-anilino group and wing II is the dibrominated phenyl group. For nevirapine, wing I is the 4-methyl-pyridine group and wing II is the other pyridine ring.

The binding of nonnucleoside inhibitors in the pocket can be likened to a butterfly resting on the β6-β10-β9 sheet and facing toward the putative entrance to the pocket (Fig. 4). The bottom of wing I has significant hydrophobic interactions with the side chains of Tyr 181 and Tyr 188. The top of wing I has hydrophobic interactions with the side chains of Trp 229 and possibly Pro 95. Wing II has fewer hydrophobic interactions compared to wing I. The bottom of wing II interacts with the side chains of Lys 101, Lys 103, Val 106, Val 179, and possibly the main chain atoms of His 235 and Pro 236. The top interacts with Tyr 318 (or Tyr 319 in the HIV-1 RT/nevirapine complex). The body of the 'butterfly' has interactions with main chain atoms of Tyr 188, Val 189 and Gly 190, and with the side chains of Val 106 and Val 179. The back of the 'butterfly' is flanked with residues Leu 100 and Leu 234, which have interactions with both wings. The side chains of these two residues are oriented directly toward the centre of the pocket, greatly decreasing its solvent-accessible space, which may help constrain the bending angle between the two wings and define the position and orientation of inhibitors within the pocket. Phe 227, located at the tail of the 'butterfly', has few contacts with the bound inhibitor but has aromatic–aromatic interaction with Tyr 188 which could influence the overall structure of the NNIBP and the binding of inhibitors. The position of the β12-β13 hairpin which includes Phe 227 prevents the inhibitor from moving deeper into the pocket. The head of the 'butterfly' is flanked by the side chain of residue Glu 138 from the p51 subunit, which partially covers the entrance of the pocket and has potential interactions with both wings. The halogen atoms in α-APA and TIBO are attached to wing II and have relatively few interactions with surrounding residues. The halogen substituents in wing II might have a role in helping precisely position the orientation of inhibitors in the pocket by causing steric restrictions on the interactions with nearby pocket residues.

In order to understand the topology and structure of the NNIBP and the interactions between the bound inhibitors and surrounding residues, the volumes of the solvent-accessible cavity (with a probe of 1.4 Å radius) and the van der Waals cavity, and the molecular volumes of nonnucleoside inhibitors were calculated using the program VOIDOO (ref. 24; Table 2). The van der Waals cavity of the NNIBP is large and its volume is similar in different inhibitor complexes. The actual solvent-accessible cavity is relatively small and its volume in different HIV-1 RT/inhibitor complexes varies considerably. The residues that form the NNIBP are flexible, and even slight conformational changes in the orientation of some side chains causes significant changes in the solvent-accessible cavity of the pocket. In particular, Leu 100 and Leu 234 point their side chains into the pocket and eliminate a large portion of the solvent-accessible space within the pocket. This partly accounts for why the same pocket can accommodate so many inhibitors with relatively different structures (see later discussion). Even though the volumes of the solvent-accessible cavities differ in different HIV-1 RT/inhibitor complexes, the solvent-accessible cavities are located at the same site and conform to a similar butterfly-like shape which is complementary to the nonnucleoside inhibitors (Fig. 2).

Table 2 Calculations of cavity and ligand volumes for HIV-1 RT/nonnucleoside inhibitor complexes

Complex[1]	Accessible cavity V (Å³)	S (Å³)	van der Waals cavity[2] V (Å³)	S (Å³)	Ligand volume V (Å³)	S (Å³)
RT/TIBO	123.9	0.4	1410	87	312.0	0.5
RT/α-APA	84.1	0.4	1513	87	343.2	0.4
RT/nevirapine	90.8	0.2	1442	83	267.4	0.4

[1]In the calculation of the volume of the nonnucleoside inhibitor-binding pocket, a dummy phenylalanine residue was modelled to cover the putative entrance of the pocket. The volumes of the cavities were measured both using a probe with radius of 1.4 Å (the accessible cavity) and without a probe (van der Waals cavity). Using ten cycles of volume calculation, a grid of 0.5 Å, and a grid-shrink factor of 0.9, all calculations for the solvent-accessible cavity converged in less than ten cycles (convergence criteria were 0.01 Å³ and 0.01%); however, the calculation for van der Waals cavity was less convergent. To assess the accuracy of the calculation, nine copies of the molecules were generated by applying randomly selected rotations around the coordinate axes. The listed values are the average volumes (V) and their standard deviations (S). For protein, all atoms were assigned default AMBER van der Waals radii; for ligands, carbons were assigned a radius of 1.95 Å, oxygens 1.60 Å, nitrogens 1.75 Å, sulphur 2.00 Å, chlorine 1.80 Å and bromines 2.05 Å.

[2]The measurement of the volume of the van der Waals cavity is not reliable and shows larger volumes than the actual cavity due to the 'can-of-worms problem' which considers the small and dendritic channels between the protein atoms as part of the cavity.

Mechanistic implications

The accumulated biochemical, structural and genetic evidence shows that many nonnucleoside inhibitors bind

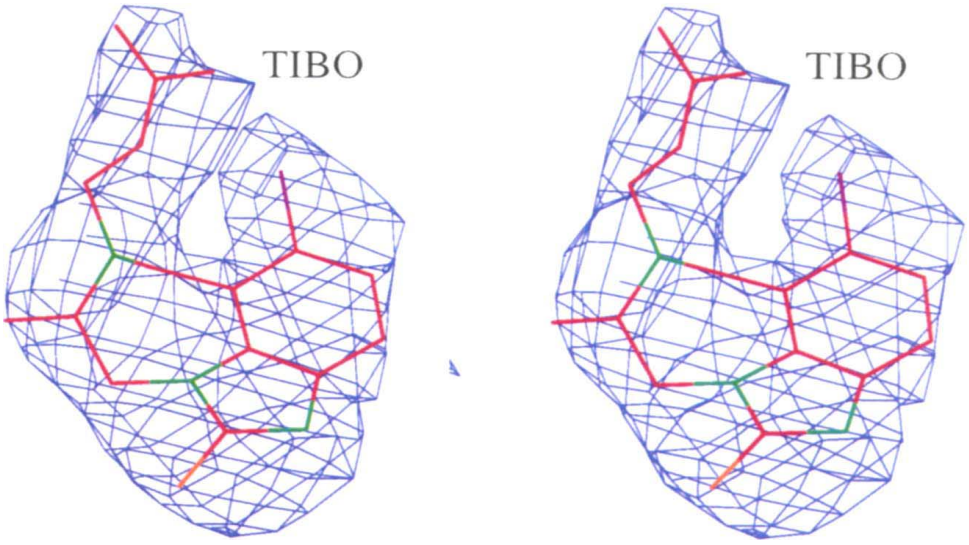

Fig. 5 Stereoview of an F_o-F_c difference Fourier map at 3.0 Å resolution (2σ contour level) showing the fit of TIBO R 86183 into the electron density. The TIBO coordinates correspond to the current refined model. The phases used were computed from a model before the TIBO inhibitor was included in the refinement.

to HIV-1 RT in a similar fashion, suggesting that they share a common mechanism of inhibition. Three possible mechanisms for the inhibition of HIV-1 RT by the nonnucleoside inhibitors have been postulated. One hypothesis is that conformational changes in the NNIBP distort the precise geometry and/or mobility of the nearby polymerase catalytic site, especially the highly conserved YMDD motif[16,18]. Mobility and flexibility at the polymerase active site appears to be essential during DNA polymerization by HIV-1 RT and other polymerases. Another mechanism is that the NNIBP functions as a 'hinge' between the palm and thumb subdomains. In this model, binding of nonnucleoside inhibitors alters the DNA-binding cleft and restricts the mobility of the thumb subdomain[16,18] which is believed to play an important role in the translocation of template-primer during DNA polymerization[20]. In addition, the β12-β13 hairpin of the p66 palm subdomain (the 'primer grip'), which forms part of the NNIBP, has close interactions with the 3'-terminus of the primer strand[20] and alteration of residues in this region, especially Trp 229, significantly impairs the polymerase activity[25](P.L. Boyer, personal communication). A third possible mechanism would be that binding of nonnucleoside inhibitors deform the 'primer grip' and consequently affects the precise positioning of the primer strand relative to the polymerase active site[18]. These possibilities are not mutually exclusive and the inhibitors may have multiple effects on the enzyme. Recent evidence from pre-steady-state kinetic analysis of HIV-1 RT inhibition by two TIBO derivatives and nevirapine suggests that nucleoside triphosphates bind tightly, but non-productively, to HIV-1 RT inhibited by nonnucleoside inhibitors[26]. These results led Spence *et al.*[26] to suggest that an inhibitor combining nucleoside and nonnucleoside moieties could be an effective inhibitor of HIV-1 RT, an idea that we initially proposed based on structural considerations[23]. The mechanisms discussed here are consistent with the kinetic data.

Nonnucleoside HIV-1 RT inhibitors are quite selective (reviewed in refs 7–9). While they are potent inhibitors of HIV-1 RT, they do not inhibit HIV-2 RT or most other retroviral RTs. When these inhibitors are used to block the replication of HIV-1, drug-resistant viral strains emerge rapidly. Mutations that confer resistance to nonnucleoside inhibitors have been identified both *in vivo* and *in vitro*, and include A98G, L100I, K101E, K103N, V106A, V108I, E138K, V179D, V179E, Y181C, Y181I, Y188H, Y188L, G190E, G190A and P236L (for recent reviews see refs 9, 27). Though relatively specific drug-resistant mutations arise in HIV-1 RT in response to different classes of nonnucleoside inhibitors, most of these mutations cause changes in amino acids that form the NNIBP and have close contacts with the bound inhibitors (Fig. 2). The exact mechanism of drug resistance to various nonnucleoside inhibitors may depend on the specific change of individual amino acid residue. Generally, alteration of these residues directly or indirectly affects the structure of the NNIBP and the stability of the binding of nonnucleoside inhibitors[9,17,18].

Binding of other nonnucleoside inhibitors

The nonnucleoside inhibitors are a diverse group of compounds with different structures, and some compounds, such as BHAP derivatives, are substantially larger than the three compounds, TIBO, α-APA and nevirapine (Fig. 1), that have been found to assume a common butterfly-like shape when bound to the NNIBP. A natural question which arises is whether the larger compounds will bind to the pocket in a similar fashion. As discussed earlier, the NNIBP is flexible and somewhat elastic and the van der Waals cavity of the pocket is large. A few hydrophobic residues point their bulky side chains into the pocket and block a large portion of the pocket from access to solvent. Some of these residues, for example Leu 100, Tyr 181, Tyr 188, Trp 229, Leu 234 and Tyr 318, have the potential to alter their side-chain conformations, changing the size and shape of the pocket. Moreover, since the NNIBP is located at the junction between the palm and thumb subdomains of p66, the conformation of the secondary structural elements that form the NNIBP could be changed in a fashion which would significantly alter the size and shape of the pocket. The β6-β10-β9 sheet is backed by helices αE and αF, and the remainder of the p66 palm. This sheet apparently moves relatively little when a nonnucleoside inhibitor binds to the pocket. The other structural components of the pocket are less constrained. The β12-β13-β14 sheet can move outward away from the pocket, since the other side of this sheet faces the solvent and there

seems to be nothing to restrict its movement. The β12-β13 loop can be pushed toward the DNA-binding cleft. In particular, if the side chain of Trp 229 is rotated away from the pocket, a large space is created that could accommodate a larger version of wing I or an equivalent part of larger inhibitors, such as the BHAP derivatives. The β5a-β6 loop is also flexible and can change its conformation to match the precise structure of the bound inhibitor. It is likely, given the flexibility of the NNIBP, that the shape of the pocket can be altered to accommodate other inhibitors whose size and shape are different.

Desiging nonnucleoside inhibitors

The crystal structures of the HIV-1 RT/TIBO, HIV-1 RT/α-APA and HIV-1 RT/nevirapine complexes show that three diverse nonnucleoside inhibitors TIBO, α-APA and nevirapine, bind to HIV-1 RT in a similar fashion. In general, most nonnucleoside inhibitors comprise two hydrophobic moieties connected by a linker group. At least one of the hydrophobic moieties, which are denoted as wing I and wing II, contains an aromatic ring with aliphatic and/or halogen substituents. The linker group usually contains atoms with tetrahedral geometry which permits the two hydrophobic moieties to be inclined at an angle of about 110°-115°.

This structural information could be used in the design of improved nonnucleoside inhibitors which would be able to inhibit some of the HIV-1 RT mutants resistant to nonnucleoside inhibitors. One possible approach in the design of more effective inhibitors might be to devise some slightly bulkier compounds containing charged or polar groups. These compounds would not only be able to fill more of the available space in the pocket, but would also be able to make specific hydrophilic interactions with the polar atoms of residues in the pocket. Another approach could be to devise compounds with functional groups which would interact with the backbone of some conserved or important residues of the pocket, such as Leu 100, Tyr 181, Tyr 188, Trp 229 and Leu 234. Strong interactions between inhibitors and the backbone of these residues could potentially overcome some of the problems caused by mutations, since mutations to residues other than proline do not change such binding sites (other than possibly leading to steric effects by residues such as Ile, Thr or Val, which are branched at the Cβ atom). It may be possible to prepare a version of wing I that would be a long, branched aliphatic group or substituted aromatic group that could make hydrophobic interactions with Trp 229. Wing II could be composed of hydrophobic and polar substituents that would be positioned to make optimal contacts with surrounding residues. The bulk of wing II should occupy the large space of the NNIBP; the hydrophobic substituent groups would make favorable interactions with the hydrophobic side chains of surrounding residues of the pocket; and the polar substituent groups could make hydrophilic interactions with the polar side chains of the hydrophilic residues around the putative entrance. A polar or charged linker group might be a good candidate which could make hydrophilic interactions with the backbone of the β6-β10-β9 sheet and stabilize the binding of inhibitor.

Although there are as yet no general methods for using structural information in the *ab initio* design of effective inhibitors, considerable progress has been made. For example a number of potent inhibitors of HIV-1 protease, some of which show promise in clinical trials, have been developed based on the structures of HIV-1 protease/inhibitor complexes[28–30]. Comparisons of these structures suggest that the pocket in HIV-1 protease where the inhibitors bind is a relatively well-conserved and fairly rigid structure among different drug complexes. This simplifies the task of drug design since the three dimensional target to which the drug should bind is relatively constant. The NNIBP of HIV-1 RT is, in contrast, a flexible structure. While this complicates the task of structure-based drug design and illustrates the importance of having a number of different HIV-1 RT structures, it may ultimately prove advantageous in designing more effective inhibitors. If, as we believe, the shape of the NNIBP is determined by its interactions with a bound inhibitor, then it may be possible that a larger number and a greater variety of compounds can bind to this pocket than would bind to a more rigid structure. This might also help explain the otherwise puzzling observation that, in random screens for inhibitors of HIV-1 replication, the vast majority of inhibitory compounds are inhibitors of RT that bind to the NNIBP.

Note added in proof: *After this paper was submitted for publication, high resolution crystal structures of HIV-1 RT in complexes with four nonnucleoside inhibitors and of unliganded HIV-1 RT were reported[32,33]. Those studies also reveal a common binding mode of diverse nonnucleoside inhibitors. The majority of conclusions drawn from those studies are consistent with the results reported here and in previous publications[17,18]. However, in the unliganded HIV-1 RT structure[32] there is only minor subdomain rearrangement but significant repositioning of a three-stranded β-sheet in the p66 palm subdomain which contains the polymerase catalytic site. These observations are different from those resulting from the structural studies of unliganded HIV-1 RT in a different crystal form[22] and of an HIV-1 RT/Fab complex (Arnold, E. et al., unpublished observations) in which the p66 thumb subdomain movement is the major change relative to the structure of HIV-1 RT containing inhibitor or DNA.*

Methods

The crystal structure of the HIV-1 RT/α-APA R 95845 complex was solved using the molecular replacement method supplemented by multiple isomorphous replacement phasing and map averaging from multiple crystal forms of HIV-1 RT/nonnucleoside inhibitor complexes. The structure was refined against 2.8 Å resolution diffraction data and converged to an *R*-factor of 25.5 % and a free *R*-factor of 36.0 % (PDB entry 1HNI)[18].

The crystal structure of the HIV-1 RT/TIBO R 86183 complex was determined using the molecular replacement method (a detailed description will appear elsewhere). The starting model for initial phasing was a full model from the HIV-1 RT/α-APA complex structure[18], which was subdivided into 13 segments and subjected to rigid body refinement. Electron density maps used for model building were calculated using the map averaging technique from multiple crystal forms of HIV-1 RT/nonnucleoside

inhibitor complexes, including the HIV-1 RT/α-APA, HIV-1 RT/TIBO and HIV-1 RT/BHAP complexes[18]. The final cycles of model building were carried out using electron density maps from a diffraction dataset from a frozen crystal of the HIV-1 RT/TIBO complex (a=225.4, b=69.4, c=104.4 Å, and β=106.4°) and from a diffraction dataset from an unfrozen crystal of the HIV-1 RT/TIBO complex (a=227.2, b=70.2, c=105.7 Å, and β=105.6°). The orientation and conformation of the TIBO inhibitor were interpreted based on the averaged difference Fourier maps (F_o-F_c) without ambiguity (Fig. 5). A difference Fourier map at 4.0 Å resolution between the HIV-1 RT complexed with a C8-iodinated TIBO analogue and the HIV-1 RT complexed with TIBO R 86183 which contains a chlorine atom on the C8 position revealed the position of the iodine atom and further confirmed the position and orientation of the TIBO inhibitor. The refinement of a current model has converged to an R-factor of 24.9 % and a free R-factor of 35.6 % using data between 10.0 and 3.0 Å resolution (26,249 and 1288 reflections with $F_o \geq 2\sigma(F_o)$, respectively). A detailed account of the structure determination and refinement of the HIV-1 RT/TIBO complex will be reported elsewhere (Das *et al.*manuscript in preparation). The coordinates of the HIV-1 RT/TIBO R 86183 complex, including the non-hydrogen atom coordinates of the TIBO inhibitor, have been deposited with the Brookhaven Protein Data Bank for immediate release (PDB tracking No. T6204).

The coordinates of the model for the HIV-1 RT/nevirapine complex used in this study were taken from the crystal structure of the HIV-1 RT/nevirapine complex which has been partially refined to 2.9 Å resolution with an R-factor of 26.6 % (free R-factor was not reported) (PDB entry 3HVT)[16,17].

Received 7 March; accepted 7 April 1995.

Acknowledgements
We thank the other members of the Arnold and Hughes laboratories and scientists at Janssen Research Foundation for their helpful discussions and assistance, including P. Boyer, A. Clark Jr., P. Clark, Y. Hsiou, L. Kaven, M. Kukla, K. Lentz, S. Mazzocchi, D. Oren, R. Pauwels, B. Roy, R. Smith, C. Tantillo, M. Zelesko, and W. Zhang. The work in E.A.'s laboratory has been supported by Janssen Research Foundation, a Johnson & Johnson Focused Giving Award, and NIH grants (AI 27690 and AI 36144). Research in S. H.'s laboratory is sponsored in part by the National Cancer Institute, DHHS under contract number NO1 CO 46000 with ABL and by NIGMS.

1. Larder, B.A. Inhibitors of HIV reverse transcriptase as antiviral agents and drug resistance. In *Reverse Transcriptase*. (eds. Skalka, A.M. & Goff, S.P), 205–222, (Cold Spring Harbor Laboratory Press, Plainview, New York; 1993).
2. Pauwels, R. *et al.* Potent and selective inhibition of HIV-1 replication *in vitro* by a novel series of TIBO derivatives. *Nature* **343**, 470–474 (1990).
3. Merluzzi, V.J. *et al.* Inhibition of HIV-1 replication by a nonnucleoside reverse transcriptase inhibitor. *Science* **250**, 1411–1413 (1990).
4. Goldman, M.E. *et al.* Pyridinone derivatives: specific human immunodeficiency virus type 1 reverse transcriptase inhibitors with antiviral activity. Proc. natn. Acad. Sci. U.S.A. 88, 6863–6867 (1991).
5. Pauwels, R. et al. Potent and highly selective human immunodeficiency virus type 1 (HIV-1) inhibition by a series of α-anilinophenylacetamide derivatives targeted at HIV-1 reverse transcriptase. Proc. natn. Acad. Sci. U.S.A. 90, 1711–1715 (1993).
6. Romero, D.L. et al. Nonnucleoside reverse transcriptase inhibitors that potently and specifically block human immunodeficiency virus type 1 replication. Proc. natn. Acad. Sci. U.S.A. 88, 8806–8810 (1991).
7. Young, S.D. Non-nucleoside inhibitors of HIV-1 reverse transcriptase. *Persp. Drug Discov. Des* **1**, 181–192 (1993).
8. De Clercq, E. HIV-1-specific RT inhibitors: highly selective inhibitors of human immunodeficiency virus type 1 that are specifically targeted at the viral reverse transcriptase. *Med. Res. Rev.* **13**, 229–258 (1993).
9. Tantillo, C. *et al.* Locations of anti-AIDS drug binding sites and resistance mutations in the three-dimensional structure of HIV-1 reverse transcriptase: implications for mechanisms of drug inhibition and resistance. *J. molec. Biol.* **243**, 369–387 (1994).
10. Frank, K.B., Noll, G.J., Connell, E.V. & Sim, I.S. Kinetics of interaction of HIV-1 RT with the antiviral TIBO R82150. *J. biol. Chem.* **266**, 14232–14236 (1991).
11. White, E.L. *et al.* A TIBO derivative, R82913, is a potent inhibitor of HIV-1 reverse transcriptase with heteropolymer templates. *Antiviral Res.* **16**, 257–266 (1991).
12. Wu, J.C. *et al.* A novel dipyridodiazepinone inhibitor of HIV-1 reverse transcriptase acts through a nonsubstrate binding site. *Biochemistry* **30**, 2022–2026 (1991).
13. Condra, J.H. *et al.* Identification of the human immunodeficiency virus reverse transcriptase residues that contribute to the activity of diverse nonnucleoside inhibitors. *Antimicrob. Agents Chemother.* **36**, 1441–1446 (1992).
14. Althaus, I.W. *et al.* Steady-state kinetic studies with the non-nucleoside HIV-1 reverse transcriptase inhibitor U-87201E. *J. biol. Chem.* **268**, 6119–6124 (1993).
15. Pauwels, R. *et al.* New tetrahydroimidazo [4,5,1-*j k*] [1,4]-benzodiazepin-2 (1-*H*)-one -thione derivatives are potent inhibitors of human immunodeficiency virus type 1 replication and are synergistic with 2',3' -dideoxynucleoside analogs. *Antimicrob. Agents Chemother.* **38**, 2863–2870. (1995).
16. Kohlstaedt, L.A., Wang, J., Friedman, J.M., Rice, P.A. & Steitz, T.A. Crystal structure at 3.5 Å resolution of HIV-1 reverse transcriptase complexed with an inhibitor. *Science* **256**, 1783–1790 (1992).
17. Smerdon, S.J. *et al.* Structure of the binding site for nonnucleoside inhibitors of the reverse transcriptase of human immunodeficiency virus type 1. *Proc. natn. Acad. Sci. U.S.A.* **91**, 3911–3915 (1994).
18. Ding, J. *et al.* Structure of HIV-1 reverse transcriptase in a complex with the nonnucleoside inhibitor α-APA R 95845 at 2.8 Å resolution. *Structure* **3**, 365–379 (1995).
19. Arnold, E., Ding, J., Hughes, S.H. & Hostomsky, Z. Structures of DNA and RNA polymerases and their interactions with nucleic acid substrates. *Curr. Opin. in struct. Biol.* **5**, 27–38 (1995).
20. Jacobo-Molina, A. *et al.* Crystal structure of human immunodeficiency virus type 1 reverse transcriptase complexed with double-stranded DNA at 3.0 Å resolution shows bent DNA. *Proc. natn. Acad. Sci. U.S.A.* **90**, 6320–6324 (1993).
21. Jager, J., Smerdon, S., Wang, J., Boisvert, D.C. & Steitz, T.A. Comparison of three different crystal forms shows HIV-1 reverse transcriptase displays an internal swivel motion. *Structure* **2**, 869–876 (1994).
22. Rodgers, D.W. *et al.* The structure of unliganded reverse transcriptase from the human immunodeficiency virus type 1. *Proc. natn. Acad. Sci. U.S.A.* **22**, 1222–1226 (1995).
23. Nanni, R.G., Ding, J., Jacobo-Molina, A., Hughes, S.H. & Arnold, E. Review of HIV-1 reverse transcriptase three-dimensional structure: implications for drug design. *Perspect. in Drug Discov. and Des.* **1**, 129–150 (1993).
24. Kleywegt, G.J. & Jones, T.A. Detection, delineation, measurement and display of cavities in macromolecular structures. *Acta Crystallogr.* **D50**, 178–185 (1994).
25. Jacques, P.S., Wohrl, B.M., Ottmann, M., Darlix, J.L. & Le Grice, S.F.J. Mutating the 'primer grip' of p66 HIV-1 reverse transcriptase implicates tryptophan-229 in template-primer utilization. *J. biol. Chem.* **269**, 26472–26478 (1994).
26. Spence, R.A., Kati, W.M., Anderson, K.S. & Johnson, K.A. Mechanism of inhibition of HIV-1 reverse transcriptase by nonnucleoside inhibitors. *Science* **267**, 988–993 (1995).
27. De Clercq, E. HIV resistance to reverse transcriptase inhibitors. *Biochem. Pharmacol.* **47**, 155–169 (1994).
28. Wlodawer, A. & Erickson, J.W. Structure-based inhibitors of HIV-1 protease. *A. Rev. Biochem.* **62**, 543–585 (1993).
29. Lam, P.Y.S. *et al.* Rational design of potent, bioavailable, nonpeptide cyclic ureas as HIV protease inhibitors. *Science* **263**, 380–384 (1994).
30. Dorsey, B.D. *et al.* L-735,524: the design of a potent and orally bioavailable HIV protease inhibitor. *J. med. Chem.* **37**, 3443–3451 (1994).
31. Carson, M. Ribbon models of macromolecules. *J. molec. Graphics* **5**, 103–106 (1987).
32. Ren, J. *et al.* High resolution structures of HIV-1 RT from four RT-inhibitor complexes. *Nature struct. Biology* **2**, 293–302 (1995).
33. Esnouf, R. *et al.* Mechanism of inhibition of HIV-1 reverse transcriptase by non-nucleoside inhibitors. *Nature struct. Biology* **2**, 303–308 (1995).